Deactivation Mechanism of ZSM-5 during Catalytic Steam Cracking of *n*-Hexane

Aritomo Yamaguchi, Dingfeng Jin, Takuji Ikeda, Koichi Sato, Norihito Hiyoshi, Tomoya Inoue, Masayuki Shirai, Fujio Mizukami, and Takaaki Hanaoka

Research Center for Compact Chemical System, National Institute of Advanced Industrial Science and Technology (AIST), 4-2-1 Nigatake, Sendai 983-8551, Japan

Introduction

Ethylene, propylene, and other light olefins are currently produced from naphtha by steam cracking at the temperature over 1073 K; however, its process requires large amount of energy because of the high reaction temperature and it is difficult to control the selectivity of the olefins. Catalytic steam cracking of naphtha has been developed using acidic catalysts, especially ZSM-5 catalysts, for higher yields of the light olefins at temperatures much lower than the steam cracking.[1-3] Although the catalytic steam cracking has distinctive advantages, it has not been widely used in commercial olefin production from naphtha because of the deactivation of the catalysts. In this paper, we investigate deactivation mechanism of ZSM-5 during the catalytic steam cracking of *n*-hexane.

Experimental

Catalytic steam cracking was carried out in a packed-bed reactor. ZSM-5 (H-ZSM-5, JGC Catalysts and Chemicals Ltd., SiO_2/Al_2O_3 = 50, 0.2 g, pellet diameter 0.5-1 mm) were diluted with quartz (1 g). These samples were placed within a quartz tube (10 mm diameter) with a K-type thermocouple enclosed in a quartz sheath in contact with the catalyst bed. H_2O and *n*-hexane were introduced using syringe pumps into the reactant stream by vaporizing into a stainless line kept at 423 K. All transfer lines from the injection point to the gas chromatograph were kept above 423 K to avoid condensation. Internal standard for gas chromatography analysis N_2 was metered by an electronic flow controller. The concentrations of reactants and products were measured by on-line gas chromatography using a MolecularSieve 13X column (for N_2, CO, and methane) and a PorapakTypeQ column (for CO_2, methane, ethane, and ethylene) with a thermal conductivity detector and using an SP1700 column (for methane, propane, propylene, *n*-butane, *i*-butane, *n*-pentane, and *n*-hexane) and a Gaskuropack54 column (for methane, *n*-heptane, benzene, toluene, and xylene) with a flame ionization detector. Conversion and product yield based on carbon are defined as given below,

Conversion (%) = 100 - (mol of unconverted *n*-hexane in products)/(mol of reactant *n*-hexane)×100 (1),

Product yield based on carbon (C%) = (mol of carbon atom in product)/(mol of carbon atom in reactant *n*-hexane)×100 (2).

The ZSM-5 catalysts were characterized by powder X-ray diffraction, solid-state magic-angle-spinning (MAS) NMR, temperature programmed desorption of adsorbed NH_3, and nitrogen adsorption analysis.

Results and Discussion

Figure 1 shows the conversion of *n*-hexane steam cracking over the ZSM-5 catalyst. The reaction temperature is 923 K and WHSV(hexane) 11 h^{-1}, W/F 8.0 g-cat h/mol-hexane, H_2O/hexane 1.0 wt/wt, P_{hexane} 14 kPa, P_{H2O} 69 kPa, and P_{N2} 18 kPa. The conversion of *n*-hexane by (thermal) steam cracking at the reaction condition was 30% as measured without the ZSM-5 catalyst (dashed line in Figure 1). The conversion of *n*-hexane over the ZSM-5 catalyst decreased from 80 to 40% with time on stream from 1 to 15 h, indicating that the ZSM-5 catalysts deactivated during the reaction. We measured the *n*-hexane conversion over the ZSM-5 catalyst pretreated with a H_2O flow (69 kPa) at 923 K for 10 h to decide whether deactivation reflects dealumination of the ZSM-5 zeolite by steam or coke formation during the catalytic steam cracking. The ZSM-5 catalyst pretreated with a H_2O flow showed 48% of *n*-hexane conversion at the beginning of reaction (Figure 1), which was much lower than that over the ZSM-5 catalyst (80%), implying that the deactivation of ZSM-5 was mainly caused by dealumination of the zeolite. Actually, the dealumination of the ZSM-5 by the pretreatment with a H_2O flow at 923 K for 10 h was confirmed by ^{27}Al and ^{29}Si MAS NMR spectra.

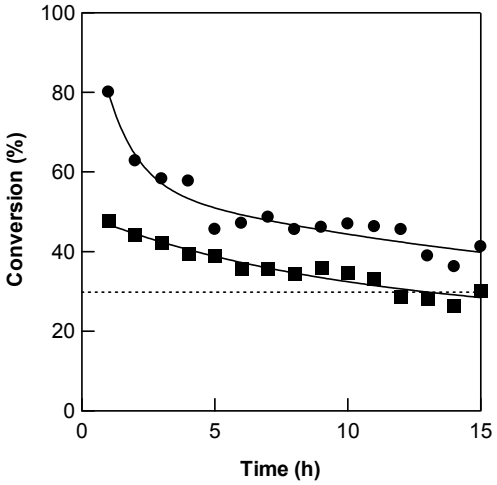

Figure 1. Conversion of *n*-hexane steam cracking over (●) the ZSM-5 catalyst and (■) the ZSM-5 pretreated with H_2O flow at 923 K for 10 h. The reaction temperature is 923 K and ZSM-5 0.2 g, quartz sand 1 g, WHSV(hexane) 11 h^{-1}, W/F 8.0 g-cat h/mol-hexane, H_2O/hexane 1.0 wt/wt, P_{hexane} 14 kPa, P_{H2O} 69 kPa, and P_{N2} 18 kPa. Dashed line indicates *n*-hexane conversion without the ZSM-5 catalyst.

References

(1) Wakui, K.; Satoh, K.; Sawada, G.; Shiozawa, K.; Matano, K.; Suzuki, K.; Hayakawa, T.; Murata, K.; Yoshimura, Y.; Mizukami, F., *Stud. Surf. Sci. Catal.* **1999,** 125, 449-456.

(2) Yoshimura, Y.; Kijima, N.; Hayakawa, T.; Murata, K.; Suzuki, K.; Mizukami, F.; Matano, K.; Konishi, T.; Oikawa, T.; Saito, M.; Shiojima, T.; Shiozawa, K.; Wakui, K.; Sawada, G.; Sato, K.; Matsuo, S.; Yamaoka, N., *Catal. Surveys Jpn.* **2000,** 4, 157-167.

(3) Wakui, K.; Satoh, K.; Sawada, G.; Shiozawa, K.; Matano, K.; Suzuki, K.; Hayakawa, T.; Yoshimura, Y.; Murata, K.; Mizukami, F., *Appl. Catal. A* **2002,** 230, 195-202.

INVESTIGATION INTO THE RELATIONSHIP BETWEEN THE GRAVITY VECTOR AND THE FLOW VECTOR TO IMPROVE PERFORMANCE IN TWO-PHASE CONTINUOUS FLOW BIODIESEL REACTOR.

Unker, S.A., Boucher, M.B., Hawley, K.R., Midgette, A.A., Stuart, J.D., Parnas, R.S.

191 Auditorium Road, Storrs, CT 06269

Introduction

Background. The production of biodiesels, or alkyl esters, has recently garnered attention due to an increasing interest in alternative fuels (*1*). Biodiesel fuel is non-toxic, biodegradable, and can be used in most diesel engines with little or no modification (*2*). Biodiesel is typically prepared via an acid or base catalyzed reaction between vegetable oil triglycerides and methanol (*3*).

Chemical processing strategies for biodiesel conversion date back to the 1940's, and are described in a series of patents by researchers from E.I. duPont and Colgate–Palmolive–Peet (*4,5*). Smaller plants often use batch reactors, but larger plants (1 million gallons/year or greater) use continuous flow processes involving continuous stirred-tank reactors (CSTR) or plug flow reactors (*6*).

In recent years, a number of continuous reactor strategies have been developed to synthesize biodiesel (*7, 8, 9, 10, 11, 12, 13*). Transesterification conversion can be enhanced by the continuous removal of the products during the reaction. There are several existing biodiesel reactor technologies that are capable of simultaneously removing the glycerol phase and driving the reaction to conversions exceeding 99%. Those designs are generally very energy intensive and may require highly elevated temperatures and pressures. Two strategies that are currently employed to accomplish that are a continuous centrifuge (*14*) and reactive distillation (*10, 15*). The former requires additional equipment and energy costs associated with their operation while the latter introduces substantial energy costs from the vaporization of lighter components. Membrane reactors have also shown promise in continuously separating methanol, biodiesel, and glycerol from the reaction mixture (*16*).

The reactor described below boasts no moving parts. The reactor also eliminates a time consuming step by combining the reaction and separation into one unit-operation.

Reactor/Separator Operating Concept. A detailed description of the reactor operating concept can be found in U.S. patent # 7,544,830 (*17*), and a recent study done by Boucher et al., 2009 (*18*). Ideally, the laminar flow reactor / separator achieves high conversion (>99%) and simultaneously separates glycerol by allowing the droplets to settle to the bottom of the reactor as the reacting flow travels upwards. The settling of particles and droplets consisting of a single material through a fluid of another material is well described by equation 1 below (*19*):

$$v_s = v_f \sin\theta - \frac{(\rho_h - \rho_l) g d^2}{18\mu} \quad (1)$$

where, v_f and v_s represent the upward velocity of the lower density oil and the downward settling velocity of the higher density glycerol, respectively. The angle θ represents the angle of the reactor column with respect to the horizontal, as shown in Figure 1(a). The settling velocity is a function of the difference in densities of the liquids (ρ_h-ρ_l), the viscosity of the lower density liquid (μ), and the diameter of the higher density droplet (d). This equation assumes that the settling particles are rigid and spherical thereby limiting its quantitative usefulness (*19*). In the present case of a two-phase liquid system, equation 1 is sufficient to indicate the major parameters controlling glycerol settling through an oil phase consisting of reacting vegetable oil and biodiesel methyl esters. The angle, θ, of the reactor with respect to the horizontal affects the vertical velocity component of the flowing bulk reaction mixture, which is opposite the gravity vector and glycerol droplet settling. Changing the vertical component of the bulk velocity, given by the term $v_f \sin\theta$ in equation 1, should affect glycerol separation, and this hypothesis is tested below.

Materials and Methods

Equipment Setup. A schematic and picture of the experimental setup are shown in Figure 1 below. The equipment consists of three main components labeled 1-3 in Figure 1(b). The core reactor, labeled 1, is composed of a 1.2 m glass column with a 15 cm ID and an 18 cm OD. The glass column is enclosed by two brass end-caps each equipped with an o-ring and three female threaded holes. An injection unit was attached to the bottom end-cap. The injection unit comprised a 15 cm static mixer with a 2 cm ID and a metal disk with holes used to cover the exit of the static mixer and disperse the flow radially. A 190 L sealed PVC tank, labeled 2 in Figure 1(b), was used as a mixing and storage unit for the potassium hydroxide-methanol solution (methoxide). The tank was kept in a chemical safety hood equipped with an extractor fan. The largest piece of equipment was a 450 L water heater (Vangaurd 240/280 Volts) labeled 3 in Figure 1(b). The water heater was used for heating the raw oil feedstock and was equipped with two heating elements. The water heater was equipped with an on/off control system to keep the feed temperatures consistent throughout the experiment.

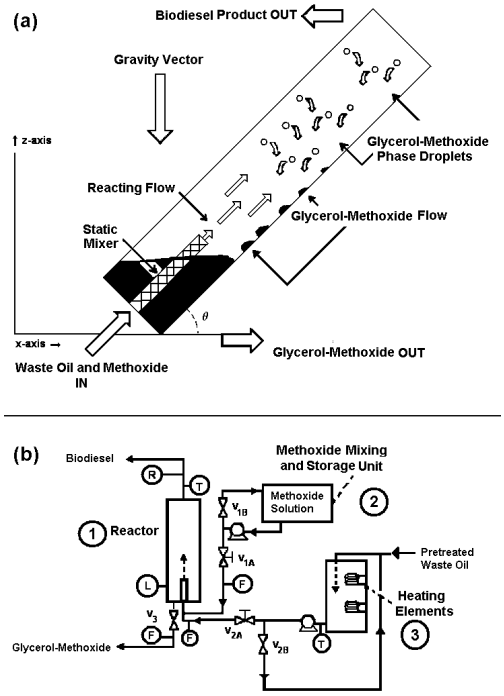

Figure 1. (a) Reactor operating concept (b) Schematic of the reactor system.

The temperature, liquid phase level, and flow rate were measured at several locations throughout the apparatus as indicated in Figure 1(b), by T, L, and F, respectively. Both thermocouples and

flow meters were equipped with digital readouts. A data acquisition card was used to record temperatures and flow rates every minute (National Instruments PCI-6221 DAQ board with a SCC-68 I/O connector block.) The flow rates of methoxide and waste vegetable oil were digitally controlled with electronic proportional valves (Hass Manufacturing Company) designated V_{1A} and V_{2A}. A computer control system developed in the LabVIEW environment employed a PI algorithm to control the inlet flows of the feedstocks. A metering valve noted V_3 in Figure 1(b) was used to manually control the flow rate of glycerol exiting the bottom of the reactor. The reactor was mounted on a hand truck to facilitate the tilting of the entire reactor column.

Feestock Preparation. Waste vegetable oil, (630 L) was collected from University of Connecticut dining halls, and Pratt & Whitney dining halls. Waste vegetable oil was filtered, blended, and titrated to measure free fatty acid (FFA) content. The feedstock which contained approximately 3 wt% FFA was pretreated by esterifying the FFA's to less than 0.5 wt%. This was achieved by an esterification reaction with methanol using hydrochloric acid (HCl) as a catalyst. The waste vegetable oil was treated in three 210 L batches. In each batch, methanol (50 L) and 36% HCl (1 L) were added to the waste oil. The batches were circulated to provide agitation and the mixture was allowed to react for 6 hours at ambient temperature. Ambient temperature was used for convenience, and previous work indicates that higher temperature requires a much shorter pretreatment time. HCl and unreacted methanol were recovered from the first batch after settling, and used again to treat the second and third batches following the same procedure. The recovered methanol layer containing the HCl contained some water from esterification; however, due to its tolerance for water, the HCl could be reused to catalyze the FFA esterification in the remaining 210 L batches. (*20*) All the esterified (pretreated waste oil) batches were blended together after the reaction was complete to ensure a uniform feedstock.

Pretreated waste vegetable oil was added to the 450 L water heater where it was circulated by a positive displacement pump (Tuthill pump Co., Aerovox motor 370 V) and heated to 50 °C. Methanol (115 L) was added to the 190 L storage tank which was set in a chemical safety hood. 6 kg of potassium hydroxide (KOH) flakes (Oxychem 88 wt% Caustic Potash Anhydrous) were dissolved into the methanol over a period of 30 min. The solution was agitated with a variable speed 115 V motorized mechanical impeller and simultaneously circulated in full recycle with a positive displacement pump (Tuthill pump Co., Aerovox motor 370 V) to aid the dissolution of the KOH flakes. Methoxide was replenished using the same relative amounts of methanol and potassium hydroxide throughout the experiments.

Starting the Reactor. Before pumping reactants into the reactor, the reactor was primed by filling it with B100 methyl esters (21 L) at room temperature. The reactant flows were started in full recycle mode, by setting the valves labeled $V_{1A,B}$ and $V_{2A,B}$ in Figure 1(b) to direct all methoxide and waste vegetable oil back to their respective storage tanks. Valve V_{2A} was then changed to direct waste oil to flow to the reactor and its flow was adjusted to the desired value by the LabVIEW control system. Immediately after, methoxide was allowed to flow to the reactor by adjusting valve V_{1A}. The flows were continuously monitored and the electronic proportioning valves V_{1A} and V_{2A} were automatically adjusted by the control system to maintain the desired flows of vegetable oil and methoxide.

Data Collection. After the flows were started, the inlet flow rates and the temperatures at the entrance and exit of the reactor were automatically recorded to file every minute by the LabVIEW control system. The temperature at the outlet of the water heater was recorded manually. The flow of glycerol exiting the bottom of the reactor was measured indirectly by maintaining a constant level of glycerol 10 cm above the reactor bottom (5 cm below the point of injection). The level of separated glycerol was maintained within ± 1 cm by manually adjusting the valve labeled V_3 in Figure 1(b). Glycerol was allowed to flow continuously into a 5 L graduated container, and time was recorded when the glycerol level reached each of the 1 L graduations. Every hour the glycerol flow rate and density were measured using a tared, 1 L graduated cylinder. The flow rate of the biodiesel product was measured using a graduated collection tank. Biodiesel product was allowed to flow continuously into the collection tank, and time was recorded each time the liquid level reached a 2.5 gallon graduation. Every sixty minutes the biodiesel flow rate and density were measured using a tared, 1 L graduated cylinder.

The first samples were taken one hour after startup. 50 ml samples were drawn every hour from both the top and bottom reactor outlets. Samples drawn from the top outlet were immediately quenched with 5 drops of 36% HCl (Sigma Aldrich reagent grade) and refrigerated. Samples drawn from the top of the reactor were centrifuged. The ester rich phase was washed with water, dried over anhydrous sodium sulfate, and prepared for gas chromatography (GC) by ASTM method D 6584-08. The samples were further analyzed by Raman (Real Time Analyzer's Fourier Transform Raman Spectrometer with InGaAs detector, 1W CW 1064 nm Nd:YAG laser at 500mW, and infotonics 316 SS probe).

Samples drawn from the bottom outlet of the reactor were sealed and kept refrigerated to avoid evaporative loss of methanol. Each bottom sample was then analyzed by thermal gravimetric analysis (TGA) using a high resolution Q500 TGA equipped with a 0-200 mg microbalance. Three drops of each sample was placed in a platinum TGA dish using a Pasteur pipette. The samples entered a sealed temperature controlled chamber filled with argon gas where the temperature was ramped from room temperature to 600 °C at a rate of 10 °C per minute. As the temperature increased, the change in mass of the sample was recorded every 0.5 s. This method is particularly effective for analyzing the mass percent of methanol in the glycerol stream because methanol and glycerol boil at widely different temperatures. Separate samples containing 88 wt% KOH were also analyzed to verify that KOH does not decompose below 600°C.

The glycerol samples were titrated to determine their KOH content using 1.0 M sulfuric acid. Titration solutions were prepared by mixing 0.3 g of sample with 5 mL of DI water and titrating with 1.0 M sulfuric acid (*21*). Control titrations were conducted using HPLC grade methanol (JT Baker), reagent grade glycerol (Acros), and reagent grade KOH (88 wt% JT Baker).

Results and Discussion

The present study contains data from three separate experiments. These experiments implemented a more effective temperature control system than previous experiments. (*18*) In all cases, the reactor was operated using pretreated waste vegetable oil as the feedstock. The pretreated waste vegetable oil was heated to approximately 50 °C and fed to the reactor at 0.95 L/min while room temperature methoxide was fed at 0.22 L/min. For the first two experiments potassium hydroxide concentration entering the reactor was 1.3 wt% with respect to triglyceride concentration in the waste vegetable oil, for the third experiment potassium hydroxide was at 1.0 wt%. These are typical catalyst loadings as published in the literature. (*22, 3*) Flows were maintained at a constant rate by a PI control system.

Reactants were pumped into the reaction vessel through a Y-joint, and then through the static mixing unit extending into the

bottom of the reactor. Biodiesel product was continuously removed from the top of the reaction vessel while glycerol was continuously removed from the bottom. The accumulating glycerol layer was maintained at a steady level below the injection point. Samples were drawn every hour during operation of the reactor from both the top and bottom outlets. Top samples were analyzed by the Raman spectrometer upon exiting the reactor. Top samples were further analyzed by gas chromatography to obtain mass percentages of triglycerides, and free and total glycerin. Bottom samples were analyzed for methanol, glycerol, and potassium hydroxide content by use of thermal gravimetric analysis and titrations.

Reactor performance was assessed by calculating both the conversion of triglycerides to methyl esters, and the simultaneous glycerol separation efficiency. The conversion of vegetable oils to biodiesels is comprised of three sequential steps [R1]-[R3], where TG, DG, and MG represent tri-, di-, and monoglycerides, respectively. G represents glycerol, and FAME represents fatty acid methyl esters or biodiesel.

$$[R1]\ TG + MeOH \overset{catalyst}{\Leftrightarrow} DG + FAME$$

$$[R2]\ DG + MeOH \overset{catalyst}{\Leftrightarrow} MG + FAME$$

$$[R3]\ MG + MeOH \overset{catalyst}{\Leftrightarrow} G + FAME$$

Assuming that the reaction [R1], TG→DG, is the rate limiting step, conversion can be expressed by equation (2).

$$x = \frac{[TG]_0 - [TG]}{[TG]_0} \quad (2)$$

where $[TG]_0$ represents the concentration of triglycerides in the feedstock (mass/volume), and [TG] represents the concentration of triglycerides in the ester rich phase exiting the top of the reactor (mass/volume). Concentration of triglycerides in the stream exiting the top of the reactor, [TG], was measured using gas chromatography and $[TG]_0$ was calculated from the density of the feedstock, accounting for the fraction of free fatty acids and methyl esters in the feedstock resulting from the pretreatment operation.

The separation efficiency was calculated using equation (3). Separation efficiency is defined as the ratio of glycerol leaving the bottom of the reactor, $F_{G\text{-}S}$, to the total glycerol produced by reaction, $F_{G\text{-}P}$. $F_{G\text{-}P}$ is a theoretical calculation using the chemical conversion to predict the maximum amount of glycerol produced by reaction.

$$separation\ efficiency = \frac{F_{G-S}}{F_{G-P}} \quad (3)$$

The stoichiometry of the transesterification reactions, R1-R3, require that 1 mole of glycerol be produced for every 3 moles of methyl esters produced. For the cases here, where very few intermediate diglycerides and monoglycerides remain in solution, the stoichiometric relationships are closely approximated by requiring 1 mole of glycerol to be produced for every mole of triglyceride consumed. Thus, the chemical conversion from equation 2 provides an accurate estimate of the maximum amount of glycerol produced by reaction, $F_{G\text{-}P}$.

Experiment 1. The first experiment assessed reactor performance in two segments. The first eight hours of continuous operation were used to repeat and verify a previously reported experiment with this reactor/separator (*18*). During the final four hours the reactor was tilted on a 45 degree angle which changed the relationship between the fluid flow vector within the reactor and the gravity vector as shown in Figure 1(a).

Figure 2 below is a triple plot displaying reactor conversion, separation efficiency, and temperature all against time. The reactor was tilted from 90 degrees to 45 degrees after approximately eight hours, ($t_{45\text{-}1}$=480 minutes) and the experiment concluded after approximately 11 ½ hours ($t_{end\text{-}1}$=690 minutes). The conversion of vegetable oil triglycerides consistently exceeded 0.99. The one outlaying data point at 640 minutes had a lower conversion due to a lower concentration of catalyst in the entering methoxide. Approximately 600 minutes into the experiment, additional methanol and potassium hydroxide were added into the large PVC "methoxide tank" to replenish the methoxide supply. 18 Liters of methanol were added to the tank first, followed by 1.08 kg of potassium hydroxide. This resulted in a lower concentration of potassium hydroxide in the methoxide tank for a brief period of time leading to the lowered conversion.

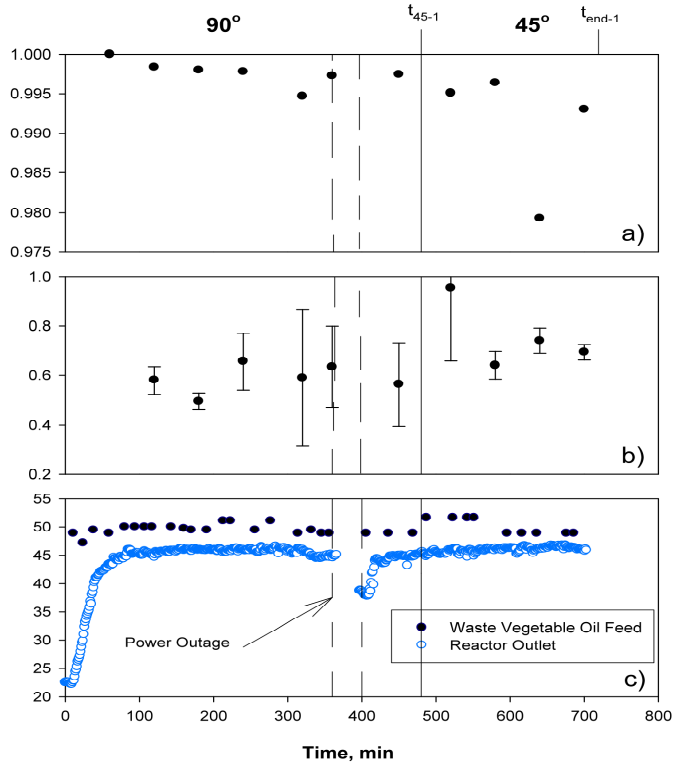

Figure 2. Results from Experiment 1. a) Triglyceride conversion according to Equation 2, b) Glycerol separation efficiency according to Equation 3, and c) Feedstock temperature and reactor outlet temperature. $t_{45\text{-}1}$ is the time the reactor was tilted from 90 to 45 degrees orientation, and $t_{end\text{-}1}$ is the time experiment 1 ended.

Separation efficiency consistently exceeded 50%. The large error bars correspond to the standard error in the measurement of the glycerol-methoxide stream exiting the reactor. A noticeable increasing trend in separation efficiency is seen once the reactor was tilted to 45 degrees with respect to the horizontal x-axis. The separation efficiency averaged over the first seven hours is 0.62, and the separation efficiency averaged over the final four hours is 0.86, although this difference is obscured by the large error bars.

Temperature of the waste vegetable oil entering the reactor was held within ± 2 degrees of 50 degrees Celsius, which was an improvement from a previous experiment (18). The reactor outlet temperature was within ± 1 degree of 46 degrees Celsius for the

majority of the experiment. The methoxide entering the reactor stayed at room temperature (approximately 25 degrees Celsius.) The previous experiment preheated the waste vegetable oil feed to approximately 65° Celsius, but over the course of the experiment, the feed temperature fell below 60° Celsius. The temperature fluctuations in the previous experiment led to the hypothesis that the separation efficiency is a strong function of temperature.

The current study shows much more consistent conversion and separation efficiency values than the previous experiment. The more consistent reactor operation in the current study illustrates the importance of temperature control. The quantitative differences between the previous and current studies are likely due to differences between the waste oil feedstocks.

As labeled in Figure 2, there was an unexpected power outage 366 minutes into the experiment, which resulted in the entire system being shut down for approximately 30 minutes. Due to the power outage, the system was restarted with the reactor at 90 degrees (vertical), and run for 60 minutes to reestablish steady operation. The climbing reactor outlet temperature from 400-425 minutes is a result of the system being shut down and restarted. The conversion and separation efficiency reported at 450 minutes, shortly before tilting the reactor, illustrates the return of reactor performance to a similar state as that established prior to the power outage. Then, the reactor was tilted to 45 degrees to obtain the data displayed in Figure 2 under the label, "45°."

Experiment 2. The second experiment was run in three segments. For the first three hours ($t_{45\text{-}2}$=200 minutes) the reactor was run with the column perpendicular to the floor as in previous experiments (θ = 90°). This was done to startup the reactor, as well as to reproduce data from experiment 1. The next six hours of reactor operation were with the column at a 45 degree angle with respect to the horizontal in order to obtain a more definitive set of data at these conditions ($t_{30\text{-}2}$ =560 minutes). The final 3 ½ hours of operation were run with the column at a 30 degree angle with respect to the horizontal in order to further investigate the relationship between reactor angle and glycerol-methoxide settling velocity ($t_{end\text{-}2}$ =750 minutes).

It should also be noted that for this second experiment, several improvements were made to the experimental setup. A second static mixer of 1.27 cm OD, and 41.5925 cm in length (koflo corporation) was added downstream of the Y-joint, but prior to entry into the column. Also, a digital flow meter was attached to the bottom (glycerol) outlet stream of the reactor and integrated into the data acquisition software. Lastly, a fiber-optically coupled Raman spectrometer was mounted (indicated by an R, in figure 1(b)) into the biodiesel outlet stream of the reactor to obtain real-time Raman measurements, to be discussed in a subsequent paper.

Figure 3 displays the experimental results for experiment 2. During 90 degree operation, conversion exceeded 0.99. As seen in experiment 1, the conversion starts out quite high because the reactor is primed with pure methyl esters. Upon tilting to 45 degrees, the conversion fell below 0.99, but held constant just below 0.99. Upon tilting the system to 30 degrees, the conversion dropped once more, but then climbed back up close to 0.99 where it held for the remainder of the experiment.

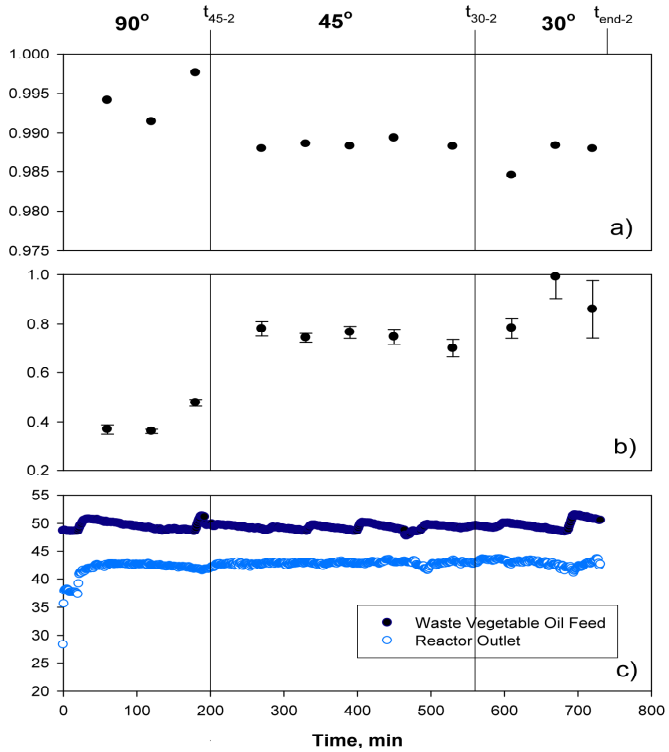

Figure 3. Results from Experiment 2. a) Triglyceride conversion according to Equation 2, b) Glycerol separation efficiency according to Equation 3, and c) Feedstock temperature and reactor outlet temperature. $t_{45\text{-}2}$ is the time the reactor was tilted from 90 to 45 degrees, $t_{30\text{-}2}$ is the time the reactor was tilted from 45 to 30 degrees, and $t_{end\text{-}2}$ is the time experiment 2 ended.

Separation efficiency in experiment 2 followed a trend similar to experiment 1. Upon tilting the reactor to 45 degrees, separation efficiency increased and held steady. The error bars on the calculated separation efficiency values in experiment 2 are much smaller than in experiment 1. This can be attributed to the digital flow meter which was attached to the glycerol-methoxide outlet stream. Once the reactor was tilted to 30 degrees, separation efficiency climbed once more. Of all the terms used to calculate the separation efficiency of the byproduct glycerol, the flowrate of the glycerol-methoxide stream is paramount. Table 1 displays the mass flowrate of this stream averaged over 20 minutes, 10 minutes before and 10 minutes after each data point. Table 1 also displays the composition in mass percentages of the glycerol-methoxide stream.

Table 1 shows the increase in the mass flow of the glycerol rich bottoms stream exiting the reactor after the reactor was tilted from 90° to 45°. Along with an increased mass flow rate, the composition of the glycerol rich stream returns to a value similar to that at 90° operation after a dynamic period. Therefore, a greater amount of methanol, potassium hydroxide, and glycerol is exiting the bottom of the reactor when titled to 45°. This leaves less methanol, and potassium hydroxide in the ester-rich phase. The decreased concentration of methoxide in the ester-rich phase may contribute to the small decrease of chemical conversion at 45°, and 30° operation.

Table 1. Mass flows, and weight percents of the glycerin rich stream exiting the reactor bottom for experiment 2.

	Sample Time, min	Mass Flow, g/min	Methanol, %	Glycerol, %	Potassium Hydroxide, %
90°	60	67	47	48	4.9
	120	64	47	48	5.4
	180	82	47	48	5.2
45°	270	123	40	55	5.2
	330	125	42	53	5.2
	390	124	41	54	4.9
	450	127	44	51	5.1
	530	121	45	49	5.2
30°	610	146	49	46	4.7
	670	160	44	52	4.4
	720	145	45	51	4.7

The temperature plot for experiment 2 shows an improvement over previous studies on this system. The waste vegetable oil entering the reactor was held within ±1 degree of 50 degrees Celsius. The reactor outlet temperature was within ±1 degree of 42 degrees Celsius for the entire experiment.

Experiment 3. The third 11 hour experiment was run similar to experiment 2 except that the concentration of potassium hydroxide was decreased to 1.0 wt%. For the first five hours ($t_{45\text{-}3}$=300 minutes) the reactor was run with the column vertical, the next four hours ($t_{30\text{-}3}$=540 minutes) were run with the column at a 45 degree angle, and the final two hours ($t_{end\text{-}3}$=660 minutes) were run with the column at a 30 degree angle.

Figure 4 displays the experimental results for all three experiments on a normalized time axis, defined below. In experiment 3, conversion initially dropped to 0.94 and then climbed from 0.94 to 0.97 during 90-degree operation. Upon tilting to 45 degrees, conversion in experiment 3 fell below 0.97, but stayed within a range of 0.95-0.97. Upon tilting the system to 30 degrees, conversion in experiment 3 stayed within a range of 0.95-0.96. Conversion values for experiment 3 are lower than values for experiments 1 and 2, which can be attributed to the lower concentration of KOH.

Separation efficiency in experiment 3 followed the same trend established in experiments 1 and 2. Upon tilting the reactor to 45 degrees, separation efficiency increased and held steady. Once the reactor was tilted to 30 degrees, separation efficiency climbed once more.

To compare the data from experiments 1, 2, and 3, the time was normalized in order to plot all three experiments together on the graphs illustrated in Figure 4. During the 90-degree portion of each experiment, time was normalized by dividing by $t_{45\text{-}i}$, the time when the reactor was tilted to 45 degrees, so that normalized time ran from 0 to 1. During the 45-degree portion of each experiment, time was normalized by first subtracting $t_{45\text{-}i}$, then dividing by the length of time the reactor was held at 45 degrees, $t_{30\text{-}i}$-$t_{45\text{-}i}$, and finally adding 1, so that normalized time ran from 1 to 2. During the 30-degree portion of each experiment, time was normalized by first subtracting $t_{30\text{-}i}$, then dividing by the length of time the reactor was held at 30 degrees, $t_{end\text{-}i}$-$t_{30\text{-}i}$, and finally adding 2, so that normalized time ran from 2 to 3.

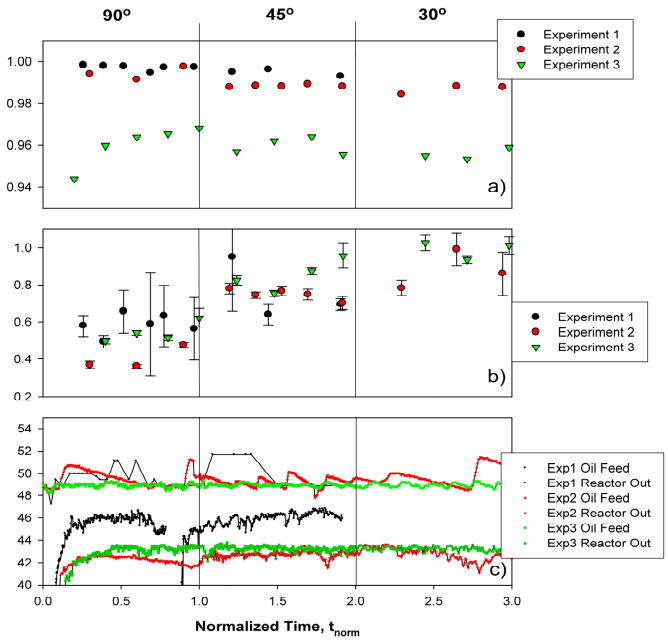

Figure 4. Results of experiments 1, 2, and 3 with time, t, normalized with respect to the times the reactor is tilted to 45, and 30 degrees, t_{norm}. a) Triglyceride conversion according to Equation 2, b) Glycerol separation efficiency according to Equation 3, and c) Feedstock temperature and reactor outlet temperature.

The chemical conversion and glycerol cleanup of the final biodiesel product are often expressed in terms of the ASTM free and total glycerin test, ASTM D 6584-08. Table 2 provides the free glycerin, total glycerin, and density results for samples drawn in all three experiments.

Table 2. Free and total glycerin (ASTM D6584-08), and density values for top samples in experiments 1, 2 and 3.

Sample	Free Glycerin, %	Total Glycerin, %	Density, g/cm^3
Exp. 1. t=320 min (90°)	0.00	0.130	0.86
Exp. 1. t=690 min (45°)	0.00	0.285	0.86
Exp. 2. t=180 min (90°)	0.00	0.097	0.86
Exp. 2. t=530 min (45°)	0.00	0.359	0.85
Exp. 2. t=720 min (30°)	0.00	0.381	0.85
Exp. 3. t=300 min (90°)	0.00	0.672	0.87
Exp. 3. t=530 min (45°)	0.00	0.950	0.86
Exp. 3. t=660 min (30°)	0.00	0.965	0.86

The data displayed in table 2 are from samples taken at the end of each experimental segment. The sample time and operating condition are listed in the first column of table 2. The density of the unwashed biodiesel is reported in table 2. Free glycerin values are all 0.00 because the samples were well washed with water to extract residual methanol, potassium hydroxide, and free glycerin, and then dried over Sodium Sulfate before GC analysis. Total glycerin values

include a weighted sum of percentages for monoglycerides, diglycerides, and triglycerides. To pass ASTM D 6584-08, free glycerin values must be below 0.020%, and total glycerin must be below 0.240%. Therefore, all samples except those from reactor configurations of 90° in experiments 1 and 2 failed the total glycerin test. This result is consistent with the conversion data presented in Figures 2, 3, and 4 since the conversion in experiment 3 was quite low due to the low value of KOH catalyst, and the conversions decreased at 45° and 30° tilt angles. Note, however, that the reactor used in this study is not an optimized design, and several design improvements can be implemented to enhance conversion with the knowledge gained in this study.

Disscussion. Separation efficiencies appeared higher in experiments 1 and 3, compared to experiment 2, especially at 90-degree operation where there is sufficient data for comparison. Our previous study suggested that the glycerol separation efficiency may be related to the temperatures observed within the reactor (*18*). Note that the reactor outlet temperature for experiment 1 was higher than in experiment 2 by roughly 4 °C. The reactor outlet temperature in experiment 3 is also slightly higher than in experiment 2, but experiment 3 also had a lower KOH concentration.

To clarify the comparison between the three experiments, compositional data was used to calculate average conversion and separation efficiency for each segment of each experiment. Data were integrated to calculate the total mass of triglycerides converted at each segment. Total glycerol separated was also calculated to show overall separation efficiencies. The averaged results are displayed in Figure 5.

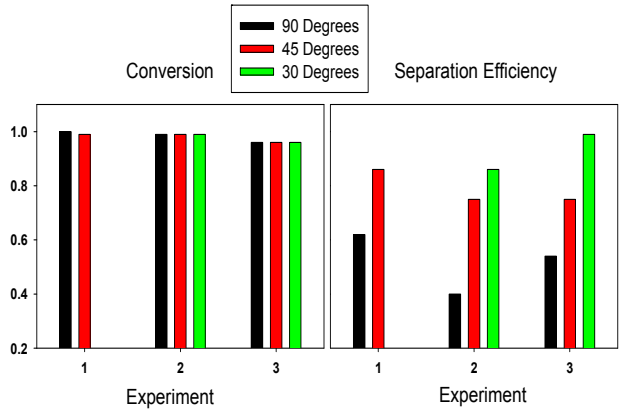

Figure 5. Conversion and separation efficiency for each set of experimental conditions.

The most striking result evident from Figures 4 and 5 is that changing reactor angle has a very large effect on glycerol separation efficiency. Equally evident is the small but non-zero effect of changing reactor angle on chemical conversion. Less evident trends in the data include probable effects of temperature and KOH concentration on conversion and separation efficiency.

It is well known that the viscosity of most fluids decreases as temperature increases. With this in mind, an inspection of equation 1 indicates that a rise in temperature that decreases the viscosity of the ester-rich biodiesel phase will lead to an increase in the glycerol droplet settling velocity. To further investigate the effects of temperature on the observed glycerol separation efficiencies, a sample of crude biodiesel exiting the reactor was taken and analyzed to measure viscosity. Viscosity was measured over a range of temperatures from 25° to 60 °C (AR-G2 Rheometer, constant shear rate = 10 s^{-1}). The viscosity changes from 0.0058 Pa●s (6.74 mm^2/s) at 25° to 0.0023 Pa●s (2.67 mm^2/s) at 60 °C, and 0.0038 Pa●s (4.42 mm^2/s) at 42° to 0.0034 Pa●s (3.95 mm^2/s) at 46 °C. This data, and many other viscosity measurements of both crude and finished biodiesel produced in this reactor from waste oil feedstocks, indicate that the biodiesel viscosity at 40 °C lies in the range of 4 – 5 mm^2/s. Thus, the biodiesel produced satisfies the ASTM D445 viscosity range of 1.9 – 6.0 mm^2/s at 40 °C.

Then, the viscosity measurements were used with equation 1 to calculate the diameter of a glycerol droplet that had a settling velocity equal to zero ($v_s = 0$). Densities of the heavy and light phases, and the bulk flow velocity used in the calculations were the measured values from the experiments. It is useful to know the size of a droplet, d_0, for which the settling velocity, v_s, is 0. Droplets that are larger than d_0 will settle ($v_s < 0$) against the bulk flow, and droplets that are smaller than d_0 will rise ($v_s > 0$) with the bulk flow.

With the reactor at 90° (vertical), the 4 °C temperature decrease from experiment 1 to experiment 2 was enough to cause a 12 micron increase in d_0. An increase in d_0 means that a larger fraction of the glycerol droplets rise with the bulk flow, and a smaller fraction settle to the bottom of the reactor. Therefore, the calculated increase in d_0 leads to a decrease in separation efficiency, and is probably the reason that a smaller separation efficiency was observed in experiment 2 than in experiment 1, at 90 degrees. While the differences in separation efficiency between experiments 2 and 3 are also consistent with this line of reasoning, the difference in temperature between experiments 2 and 3 is very small so other factors may also account for the differences observed.

These calculations also display the effect of changing the reactor angle on d_0. At a reactor temperature of 42 °C (experiment 2), changing the reactor angle from 90° to 45° leads to a decrease in d_0 from 235 microns to 197 microns. This calculated decrease in d_0 causes a larger fraction of the glycerol droplets to settle leading to the observed increase in separation efficiency, and similarly, to the further increase in separation efficiency observed when the reactor was tilted to an angle of 30°.

It was expected that the increase in glycerol separation would lead to greater chemical conversion due to shifting of (Le Chatelier's principle) chemical equilibrium. The experimental data, however, showed that the increase in glycerol separation also leads to a greater separation of methanol and potassium hydroxide, which is detrimental to overall conversion.

Conclusions

Three independent experiments were run with a newly patented novel continuous flow biodiesel reactor/separator. The experiments showed that chemical conversion is insensitive to changing the angle of the reactor, while the separation of glycerol is very sensitive to the reactor angle. Comparisons between experiments 1, 2, and 3 appear to validate hypothesis that glycerol separation efficiency is also very sensitive to reactor temperature. Experiment 3 showed the sensitivity of the reactor to catalyst concentration. Simple calculations with equation 1 made using viscosity, density and flow data explain the effects of both reactor angle and temperature on glycerol separation efficiency.

Acknowledgement. The authors gratefully acknowledge the financial support of the United States Dept. of Agriculture, the Connecticut Dept. of Economic and Community Development, and the Connecticut Center for Advanced Technology.

References

(1) Boehman, A.; McCormick, R. *Fuel Process. Technol.* **2007**, *88*, 641.
(2) Szybist, J.; Song, J.; Alam, M.; Boehman, A. *Fuel Process. Technol.* **2007**, *88*, 679.
(3) Noureddini, H.; Zhu, D. *J. Am. Oil Chem. Soc.* **1997**, *74*, 1457–1463.

(4) Dreger, E.E. Method of Treating Fatty Glycerides. U.S. Patent 2,383,596, August 28, 1945.
(5) Bradshaw, G.B.; Meuly, W.C. Process of making pure soaps. U.S. Patent 2,271,619, February 3, 1942.
(6) Van Gerpen, J. *Fuel Process. Technol.* **2005**, *86*, 1097–1107.
(7) Behzadi, S.; Farid, M.M. *Bioresour. Technol.* **1992**, *100*, 683-689.
(8) Chen, Y.; Huang, Y.; Lin, R.; Shang, N. *Bioresour. Technol.* **2010**, *101*, 668-673.
(9) Halim, S.F.A.; Kamaruddin, A.H.; Fernando, W.J.N. *Bioresour. Technol.* **2009**, *100*, 710-716.
(10) Kiss, A. A.; Dimian, A. C.; Rothenberg, G. *Energy Fuels* **2008**, *22*, 598-604.
(11) Komers, K.; Skopal, F.; Cegan, A. *Bioresour. Technol.* **2010**, *101*, 3772-3775.
(12) Stavarache, C.; Vinatoru, M.; Maeda, Y.; Bandow, H. *Ultrason. Sonochem.* **2007**, *14*, 413-417.
(13) Wen, Z.; Yu, X.; Tu, S.; Yan, J.; Dahlquist, E. *Bioresour. Technol.* **2009**, *100*, 3054-3060.
(14) Peterson, C. L.; Cook, J. L.; Thompson, J.C.; Taberski, J. S. *Trans. ASABE* **2002**, *18*, 5–11.
(15) He, B.B.; Singh, A.P.; Thompson, J.C. *Trans. ASABE* **2006**, *49*,107-112.
(16) Dube, M.A.; Tremblay, A.Y.; Liu, J. *Bioresour. Technol.* **2007**, *98*, 639-647.
(17) Parnas, R.; Weed, C.; Leadbeater, N.; Boucher, M. US Patent 7,544,830, June 9, 2009.
(18) Boucher, M.B.; Weed, C.; Leadbeater N.E.; Wilhite B.A.; Stuart, J.D.; Parnas, R.S. *Energy Fuels* **2009**, *23*, 2750-2756.
(19) Geankoplis, C.J. *Transport Processes and Separation Principles: Fourth Edition*; Pearson Educational Inc.: New Jersey, 2003; p. 902.
(20) Boucher, M.B.; Unker, S.A.; Hawley, K.; Wilhite, B.A.; Stuart, J.D.; Parnas, R.S. *Green Chem*. **2008**, *10*, 1331-1336.
(21) Zhou, W.; Boocock, D. *J. Am. Oil Chem. Soc.* **2006**, *83*, 1047–1052.
(22) Vicente, G. ; Martınez, M.; Aracil, J.; Esteban, A. *Ind. Eng. Chem. Res.* **2005**, *44*, 5447-5454.